

# Three different ways of implementing cycloidal computed tomography: a discussion of pros and cons

Oriol Roche i Morgó, Fabio Vittoria, Marco Endrizzi, Alessandro Olivo, and Charlotte K. Hagen

**Abstract**—We present three implementation strategies for cycloidal computed tomography. The latter refers to an imaging concept that enables the acquisition of high-resolution tomograms in a flexible manner (e.g. with x-ray sources with a relatively large focal spot and detectors with relatively large pixels). In cycloidal computed tomography, the sample is rotated and laterally translated simultaneously; with this scheme, each sample feature follows a cycloidal trajectory. This has been shown to reduce scanning time and delivered dose, while maintaining a high resolution. The different ways of implementing this method are: step-and-shoot, continuous unidirectional and continuous back-and-forth translation. While step-and-shoot acquisitions yields the best results and are easiest to implement, they are also the most time-consuming. The continuous unidirectional method can be implemented with little effort and gives results comparable to step-and-shoot. Finally, back-and-forth scans can be implemented easily and provide similar results, although there appears to be a small loss in image quality. We present a comprehensive guide on using cycloidal sampling in practice.

**Index Terms**— computed tomography, sampling, spatial resolution, structured illumination, x-rays

## I. INTRODUCTION

X-ray micro computed tomography (CT) is a robust imaging technique that produces high-resolution images (a few to tens of  $\mu\text{m}$ ) of a sample. The images can then be combined to visualize a slice or 3D rendering of the sample with very fine detail. [1, 2]

In order to obtain high-resolution images, specialized hardware is generally necessary, specifically a source with a sufficiently small focal spot and a detector with small pixels that suffer negligible crosstalk. These sources and detectors exist, but they are not the norm in several applications and impose a restricted field of view, respectively [3].

Higher spatial frequencies can be accessed when the x-ray beam is appropriately structured, even when the source focal

spot and detector pixels are relatively large. We have developed an approach that consists of splitting the x-ray beam into an array of narrow beamlets (a few  $\mu\text{m}$  to tens of  $\mu\text{m}$ ), the use of which allows achieving higher resolution, largely decoupled from the source and detector properties. However, in principle our approach requires a dense sampling scheme, by which the sample is scanned laterally in multiple steps at every rotation angle (a process called “dithering”) in order to ensure that each part of the sample has been illuminated by the beamlets [4]. This is an inefficient procedure that introduces dead times in the acquisition process, lengthening scan times significantly. Importantly, it is incompatible with continuous acquisitions (sometimes termed “fly scans”).

Cycloidal computed tomography overcomes this problem by under-sampling in an efficient manner and compensating the data incompleteness via a mathematical recovery method (explained in detail below).

We would also like to highlight that cycloidal computed tomography is a highly flexible concept, in the sense that it can be implemented in both attenuation and phase contrast modes (again see below). This is particularly powerful because different samples might benefit from using different contrast channels.

However, the cycloidal technique is relatively new and there has been little work on how to optimally implement it in practice. We have explored three different acquisition strategies for cycloidal computed tomography and compared them.

## II. BACKGROUND

### A. Cycloidal computed tomography [5]

Cycloidal computed tomography is enabled by combining the beamlet-based setup described above with an innovative, efficient sampling scheme, and an appropriate data recovery method.

As mentioned above, before hitting the sample the x-ray beam is split into an array of beamlets with the help of an absorbing mask (“sample mask”) with periodically spaced slit-shaped apertures (Fig. 1). There are two specific criteria for the mask: first of all, the aperture width ( $w$ ) must be smaller than

M. Endrizzi and C. K. Hagen are supported by the RAEng under the Research Fellowship scheme. A. O. is supported by the Royal Academy of Engineering (RAEng) under the Chair in Emerging Technologies scheme.

O. Roche i Morgo, M. Endrizzi, A. Olivo and C. K. Hagen are with the Department of Medical Physics and Biomedical Engineering at University College London, London, UK.

Fabio Vittoria is with ENEA – Radiation Protection Institute, Bologna, Italy. Contact: oriol.roche.15@ucl.ac.uk.

the system blur in order to access spatial frequencies higher than those usually available with the same source and detector. Secondly, the mask period ( $p$ ) must be large enough to prevent overlap between adjacent beamlets. Usually  $p$  matches the pixel size of the detector ( $a$ ) when scaled to the isocenter of the sample. However, in order to ensure the second criterion, sometimes a “line-skipping” mask is employed, which has a larger period, so that some pixels are covered and only every second pixel (or third, or fourth...) is illuminated.

Under these conditions, the cycloidal sampling scheme can be employed. The sample is translated laterally through the setup simultaneously to being rotated around the vertical ( $y$ -) axis. At each rotation angle, only a single frame is acquired. The sample is then slightly shifted as it is rotated to the next angle, another frame is acquired, and so on. This sampling scheme differs from dithering (where the sample is scanned laterally in multiple steps at each angle, see above) because at every angle only a single frame, with the sample in a slightly different lateral position, is acquired. The distance  $d$  by which the sample is translated per rotation angle is a fraction of the mask period.

With this “roto-translation” motion, the acquired data correspond to a well-spread distribution on the sinogram sampling grid (Fig. 2c). The exact data distribution depends on the value of  $d$ , as well as the angular sampling step. Although evidently the sinogram is incomplete (only the filled dots are available, all others are not acquired), this spread helps recover the missing entries, because the data points complement each other better than in the rotation-only case (Fig. 2a), where they are densely packed in the angular direction but far apart in the lateral direction. In fact, with an appropriate data recovery method (which can range from bicubic interpolation to machine learning approaches), the cycloidal sampling scheme allows accessing spatial resolutions comparable to dithering (which leads to complete sinograms, Fig. 2b) even though fewer frames are acquired.

### B. Edge-Illumination X-ray Phase Contrast

The edge-illumination (EI) x-ray phase contrast technique is a form of x-ray phase contrast imaging, developed originally with synchrotron radiation but subsequently extended for use in laboratory settings with conventional x-ray tubes [6]. Phase contrast imaging takes advantage of the phase and refraction effects introduced by a sample, in addition to the attenuation in conventional x-ray imaging. In the case of weakly attenuating materials, such as biological soft tissue, the exploitation of phase effects is known to increase image contrast. Therefore, phase contrast techniques, and the EI technique among them, present great potential in the field of biomedical imaging [7].

The beamlet-based scanner setup, which is the basis for performing cycloidal computed tomography, can easily be converted into an EI x-ray phase contrast imaging system. To do so, a second absorbing mask (“detector mask”) is placed in front of the detector (see Fig. 1). This mask also has periodically spaced apertures which match, adjusted for magnification in a cone beam system, the apertures of the first mask. The two masks are positioned with respect to each other so that, without a sample, approximately half of each beamlet falls on each side

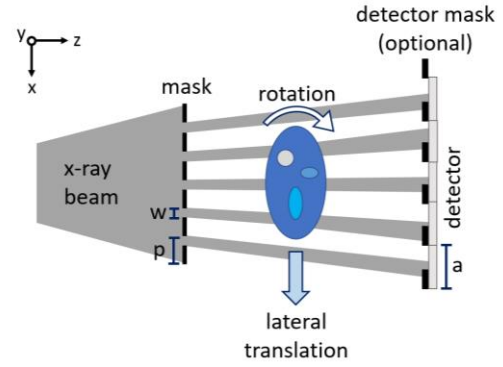


Figure 1. A schematic representation of our setup. The first mask splits the beam into beamlets. The second (optional) mask transforms the set-up into an edge-illumination system. Introducing the sample causes the beamlets to shift (due to refraction) which provides the phase contrast. By simultaneously rotating and translating the sample laterally, we can obtain cycloidally sampled datasets.

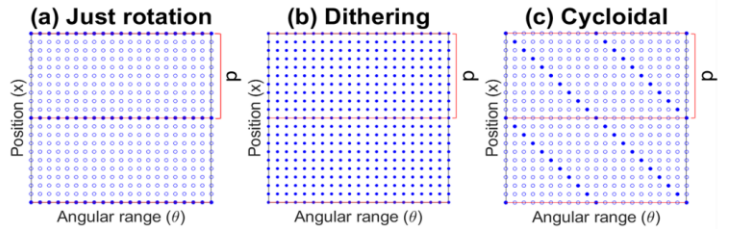


Figure 2. Sketch of the sinogram sampling grid for different sampling strategies, shown for two mask periods and a subset of rotation angles. In each panel, the filled dots represent data points that are acquired during a scan, while the empty dots represent the data that are not acquired. Panel (a) shows the grid if the sample only rotates. The data points are densely packed in one direction only. Panel (b) shows the grid when dithering is applied. The grid is fully sampled. Panel (c) shows the grid when applying a cycloidal scheme (with  $d = 0.0625p$ ). The number of data points in (c) is the same as in (a), but they are more evenly distributed across the grid.

of an edge created by the detector mask apertures, giving a specific intensity signal. When a sample is introduced, refraction slightly shifts the beamlets according to the sample’s composition and geometry, and the intensity on the detector plane changes, which gives rise to phase contrast [8, 9].

In order to accurately position the masks, usually an illumination curve (IC) is acquired by shifting the sample mask by several steps over one period and recording the intensity changes in the detector. The IC can be approximated as a Gaussian curve and used to determine the best position of the sample mask to maximize the phase signal.

When reconstructing CT images, a process called “phase retrieval” is required. This is because the intensity in a single image is the combination of attenuation and refraction effects, and a specialized algorithm is necessary to isolate the phase signal. When the sample is homogeneous, the images are acquired on one of the slopes of the IC and the beam shift is sufficiently small, only one image per projection angle is required for the retrieval process. This is referred to as a “single-shot” approach [10].

### III. PRACTICAL IMPLEMENTATION STRATEGIES

Cycloidal computed tomography can be implemented in a flexible manner. We have investigated three different options to do this: step-and-shoot, continuous unidirectional and

continuous back-and-forth scanning.

The sample was a phantom composed of polyethylene spheres between 425 and 500  $\mu\text{m}$ , contained in a 3 cm diameter plastic straw. As this sample is weakly attenuating, all data were acquired using the scanner in x-ray phase contrast mode, by implementing the EI technique. The detector was a CMOS-based flat panel C9732DK-11 with 50  $\mu\text{m}$  pixels from Hamamatsu (Japan). A “line-skipping” detector mask (with an aperture width of 17  $\mu\text{m}$  and a period of 98  $\mu\text{m}$ ) was employed to reduce the adverse effects of pixel cross talk; this has resulted in an effective pixel size of 80  $\mu\text{m}$  (at the sample plane). The sample mask had a 79  $\mu\text{m}$  period and 10  $\mu\text{m}$  aperture. The source was a MicroMax 007 HF x-ray tube with a Molybdenum target from Rigaku (Japan), operating at 40 kVp and 20 mA. The processing of all data included flat field and dark field corrections, and single-shot phase retrieval. The missing data points in the sinogram (see Fig. 2c) were recovered using bicubic interpolation.

#### A. Step-and-shoot scanning

In step-and-shoot mode, all frames are acquired by first moving the sample to position, then exposing it to x-rays and saving the detector’s response. The sample is then moved to the next (lateral and angular) position, exposed again, and so on. In our case, we only translated the sample by up to one mask period, then shifted it back to its initial position, then repeated the stepped, lateral movement by up to one mask period, and so on (see schematic in Fig. 3a). Due to the periodicity of the pixel array, this is equivalent to translating the sample along one direction only.

In a step-and-shoot scan, the distance  $d$  by which the sample is translated per angular step does not vary throughout the scan, which opens the question as to whether there is an optimal value of  $d$ . We have run tests for different values, and  $d = 0.25p$  has been found to lead to the best results in terms of spatial resolution [11].

900 frames were acquired over  $180^\circ$ , with an angular step of  $0.2^\circ$  and an exposure time of 1.1 s per frame.

#### B. Continuous unidirectional scanning

In continuous unidirectional mode, the sample starts rotating and moving laterally at the same time and does not stop until all projections have been acquired. The lateral movement is performed in just one direction, so the sample starts at one side of the field of view and moves towards the other side (see schematic in Fig. 3c). Because of this, the sinogram is “slanted” and the data points need to be re-positioned into what would be their correct pixel position if a step-and-shoot scan were acquired, in a process that we call regridding.

The continuous unidirectional data were again acquired with  $d = 0.25p$ . 900 frames were acquired over  $180^\circ$ , with an angular step of  $0.2^\circ$  and an exposure time of 1.25 s per frame. This corresponds to a total translated distance of 17.775 mm. A few extra projections (not used in the reconstruction) were acquired, to account for the acceleration and deceleration of the translation and rotation stages.

#### C. Continuous back-and-forth scanning

This acquisition strategy consists of moving the sample laterally between two points within the field of view, back and forth until all projections are acquired. In a similar way as for the continuous case above, the sinogram is “slanted” (Fig. 3e), so it also requires re-positioning the data points, or regridding.

The continuous back-and-forth data were acquired as detailed in the section above. The two endpoints of the back-and-forth motion were selected so that 500 projections could be acquired in between (which corresponds to a distance of 9.875 mm). Again, a few extra projections at the beginning and at the end of the scan were included to account for motor acceleration and deceleration, which were omitted in the reconstruction. The motor acceleration and deceleration around the point where the sample changes direction were considered negligible.

#### D. Dithered scanning

For comparison, we have also acquired a dithered, i.e. complete dataset. The dithered data were acquired with 8 dithering steps, each with 1.1 s of exposure time. A total of 7200

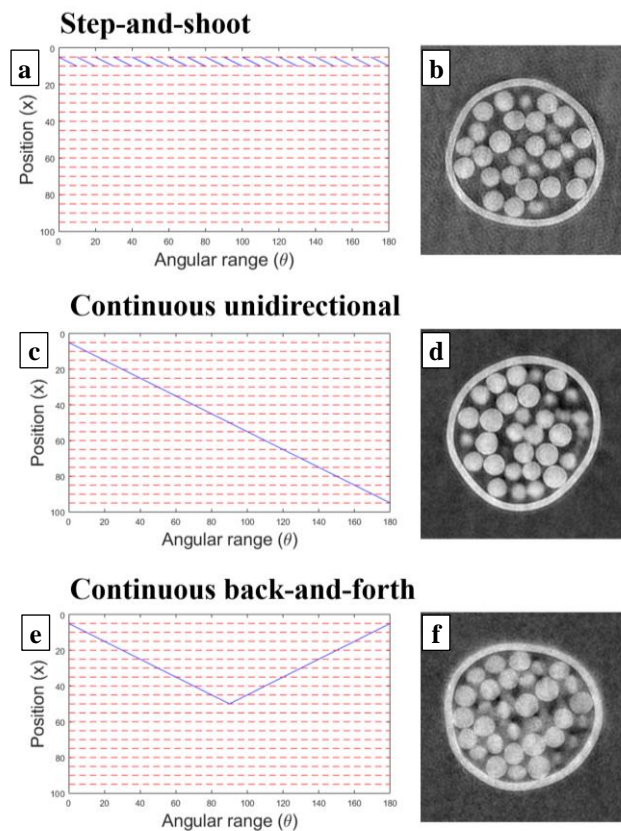


Figure 3. For the three cycloidal computed tomography implementation strategies, (a), (c) and (e) schematically show the trajectory of the sample during scans. Panels (b), (d) and (f) show the reconstructed images of the sample obtained for each implementation strategy.

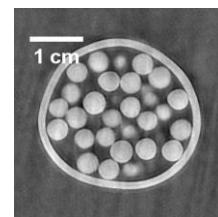


Figure 4. Reconstructed tomographic image from a fully dithered dataset with 8 dithering steps.

frames were acquired over  $180^\circ$ , with an angular step of  $0.2^\circ$ . The sinogram data were already complete (see Fig. 2b), so no bicubic interpolation or regridding was used in this case. As for the cycloidal cases, single-shot retrieval was applied.

#### IV. RESULTS AND DISCUSSION

The three strategies presented above are all realistic options for implementing cycloidal computed tomography in practice. The results obtained through the step-and-shoot and continuous unidirectional acquisitions are qualitatively similar to each other, as well as to the dithered images. This shows the potential of the method: despite acquiring a fraction of the frames compared to dithering (eight times fewer frames), we obtain comparable images, especially in terms of spatial resolution. In comparison to the step-and-shoot and continuous unidirectional scenarios, the images acquired with the continuous back-and-forth sequences appear somewhat blurrier and noisier.

Each of the presented implementation strategies exhibits advantages and disadvantages. Data acquired in a step-and-shoot fashion do not require any regridding of the sinogram before reconstruction, like in the continuous cases. This is an advantage because the regridding process is error prone (as the speed of the translation motor has to be known precisely to achieve an accurate result). On the downside, step-and-shoot acquisitions require longer scan times because the motors are stopped and started again at every step, introducing dead times.

For the continuous unidirectional scan, the continuous movement does not seem to affect the image. The regridding is relatively straight-forward as long as the translation speed of the motor is accurately known. The key advantage of continuous scans is that they can be fast (no dead times are required for stop-starting the motors), which makes unidirectional continuous cycloidal CT a powerful alternative to step-and-shoot scanning.

A drawback of the unidirectional method lies in its field of view restrictions. The field of view needs to be wide enough for the sample to move from one end to the other and include all lateral positions in that movement. For small samples (a few centimeters) this might be feasible, depending on the detector and size of the masks, but for larger samples it might be difficult to find a setup with a sufficiently large field of view.

The back-and-forth strategy offers a possible solution to this: for cases with a limited field of view, once the sample reaches the end it can turn around and continue in the other direction; this is then repeated until all frames are acquired. However, as mentioned above the back-and-forth case gives blurrier results. This might be due to additional complications in the data processing. In the back-and-forth movement, when the sample changes direction, the value of  $d$  is not constant, due to the acceleration and deceleration of the translation motor, making the regridding process more difficult. In our example, there was only one change in direction, which we have assumed to be negligible (and assumed that the position of the sample strictly follows from the  $d$  values). We suspect, though, that the effect of this erroneous assumption will increase with the number of times motion is reversed. A more accurate hardware may exist

that allows for the exact sample position to be known with much higher accuracy, which would allow for the data to be regridded more accurately, thus improving the result.

We would like to highlight that, in the extreme case, the back-and-forth method could be implemented by only moving the sample back-and-forth within one (de-magnified) pixel. In that case, there would be no need for regridding the data, and the field of view requirements would be even more relaxed, thus increasing the number of samples that could take advantage of the cycloidal method. However, this strategy requires quick acceleration and deceleration of the motors and very accurate knowledge of the sample position, so it will be the focus of future work.

#### V. CONCLUSION

In summary, we have presented three different practical implementation strategies for cycloidal computed tomography.

Both step-and-shoot and continuous cycloidal scans are relatively straight-forward to implement and provide images of comparable quality to fully dithered scans, despite the acquisition of substantially fewer projections. A key strength of the continuous approaches (unidirectional and back-and-forth scanning) is that these are much faster in terms of overall acquisition duration as they eliminate all dead times. Not only do these strategies lead to short scan times, they also have relaxed field of view requirements and provide good image quality. For these reasons, we envision the continuous acquisition strategies to become the methods of choice for applications of cycloidal computed tomography. More work to improve the image quality delivered by the presented continuous back-and-forth acquisition strategy will be performed, and variations of these strategies (such as moving the sample within one pixel) will be investigated.

#### REFERENCES

- [1] A. Kak and M. Slaney, *Principles of computerised tomographic imaging*, IEEE Press, New York, NY, USA, 1988.
- [2] E. Baird and G. Taylor, "X-ray micro computed-tomography," *Current Biology*, vol. 27, no. 8, pp. R289-R291, 2017.
- [3] J. Wan and D. Fleischmann, "Improving Spatial Resolution at CT: Development, Benefits, and Pitfalls," *Radiology*, vol. 289, no. 1, pp. 261-262, 2018.
- [4] P. C. Diemoz, F. A. Vittoria and A. Olivo, "Spatial resolution of edge illumination X-ray phase-contrast imaging," *Optics Express*, vol 22, no. 13, pp. 15514-15529, 2014.
- [5] Cycloidal Computed Tomography, by C. K. Hagen, F. Vittoria, M. Endrizzi and A. Olivo (2018, Dec 13). UK Patent Application 1820362.0
- [6] A. Olivo and E. Castelli, "X-ray phase contrast imaging: from synchrotrons to conventional sources", *La rivista del nuovo cemento*, vol 37, no. 9, 2014.
- [7] A. Bravin, P. Coan and P. Suortti, "X-ray phase-contrast imaging: from pre-clinical applications towards clinics", *Physics in Medicine & Biology*, vol 58, no. 1, 2012.
- [8] A. Olivo et al, "An innovative digital imaging set-up allowing a low-dose approach to phase contrast applications in the medical field", *Medical Physics*, vol 28, no. 8, 2001.
- [9] A. Olivo and R. D. Speller, "A coded-aperture technique allowing x-ray phase contrast imaging with low-brilliance x-ray sources", *Appl. Phys. Lett.* vol 91, no. 7, 2007.
- [10] P. Diemoz et al, "Single-shot x-ray phase-contrast computed tomography with non-microfocal laboratory sources", *Phys. Rev. Appl.* vol 7, no. 4, 2017
- [11] O. Roche, manuscript in preparation.